Danussi et al., http://www.jcb.org/cgi/content/full/jcb.201008013/DC1

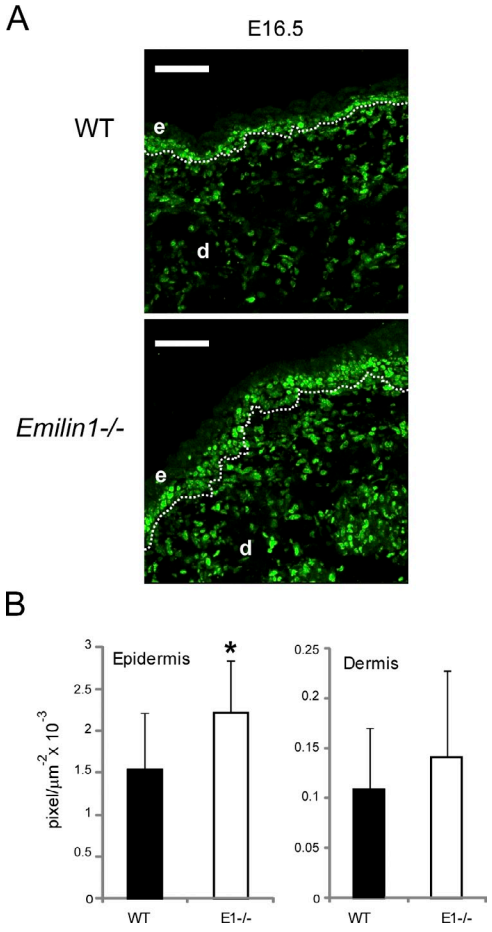

Figure S1. **Skin hyperplastic phenotype in *Emilin1*$^{-/-}$ mouse embryos.** (A) Representative images of WT and *Emilin1*$^{-/-}$ mouse skin cryostat sections at E16.5. d, dermis; e, epidermis. The dashed lines denote the BM. Bars, 75 µm. (B) ImageJ analysis of the Ki67 staining (mean of pixel/µm^2 x 10^{-3}) in WT and *Emilin1*$^{-/-}$ mouse epidermis and dermis. Mean values ± SD are reported. *, P = 0.01. For these quantitative analyses, five different cryostat sections of E16.5 WT (n = 3) and *Emilin1*$^{-/-}$ (n = 3) mice were examined.

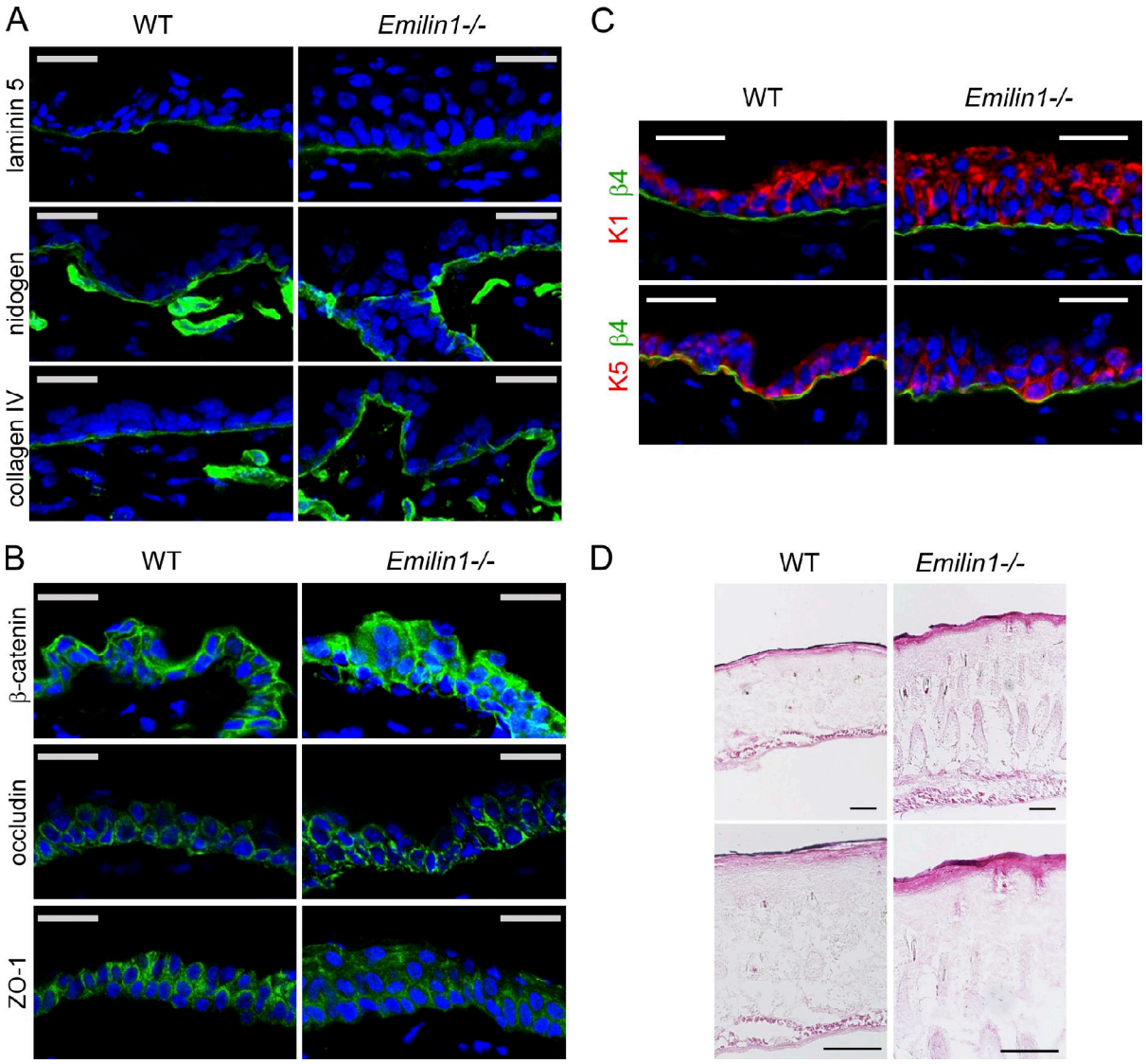

Figure S2. **Comparable expression of basal membrane/ECM, polarity and cell junctional markers, and normal barrier function of skin.** (A and B) Representative images of WT and *Emilin1*$^{-/-}$ 7-wk-old skin cryostat sections. Laminin-5, nidogen, collagen IV, β-catenin, occludin, and ZO-1 are stained in green. Nuclei are shown in blue. No appreciable differences between WT and *Emilin1*$^{-/-}$ mice were detected. Bars, 25 µm. (C) The β4 integrin chain is expressed by K5-positive keratinocytes in both WT and *Emilin1*$^{-/-}$ skin. Bars, 25 µm. (D) Barrier dye penetration assay. 4-d-old WT and *Emilin1*$^{-/-}$ mice were sacrificed with carbon dioxide and fixed for 5 min with methanol followed by incubation for 4 h in 0.5% hematoxylin. After a brief washing with water, skin pieces were dissected and snap frozen with optimal cutting temperature compound, and cryosections were counterstained with eosin. Bars, 100 µm.

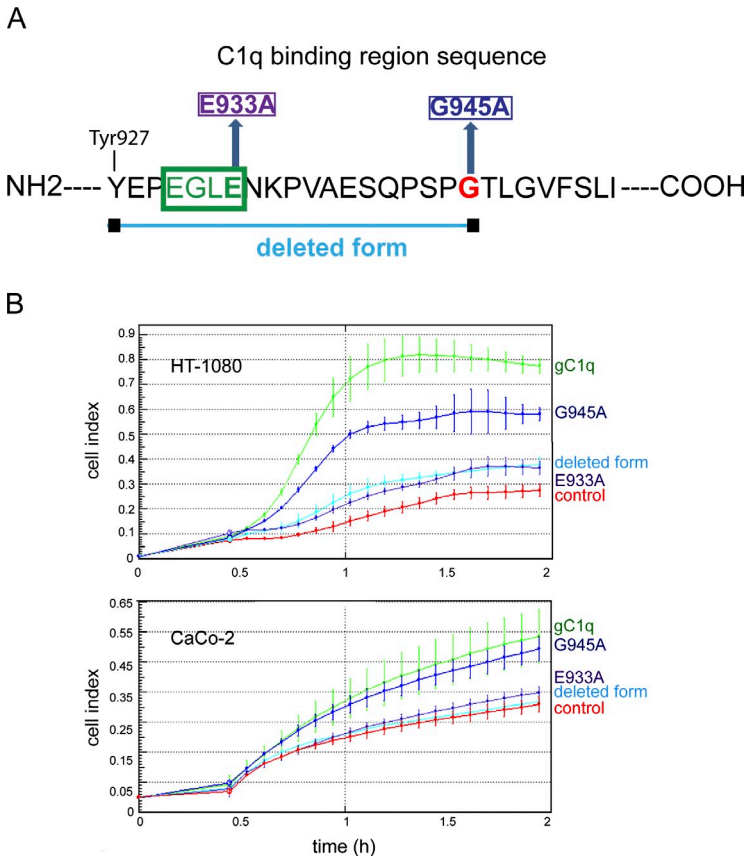

Figure S3. **gC1q mutants and their binding activity.** (A) A schematic of the mutations in the C1q binding region sequence. The position and the nature of the mutations are indicated by arrows. E933A, G945A, and deleted form (Tyr927–Gly945) mutants proved soluble and had the same thermal stability as the WT EMILIN1 gC1q, suggesting correct folding. The green boxed EGLE tetrapeptide of EMILIN1 gC1q was found to be the most relevant and important recognition sequence for $\alpha 4\beta 1$ integrin, as previously described by Verdone et al. (2008). (B) Dynamic monitoring of HT1080 and CaCo-2 cell attachment in response to gC1q domain, its mutants (G945A and E933A), and its deleted form measured with the XCELLigence instrument and expressed as the cell index. The control corresponds to cells adhering to plastics. The data shown are the mean ± SD from $n = 3$ experiments with $n = 6$ replicates.

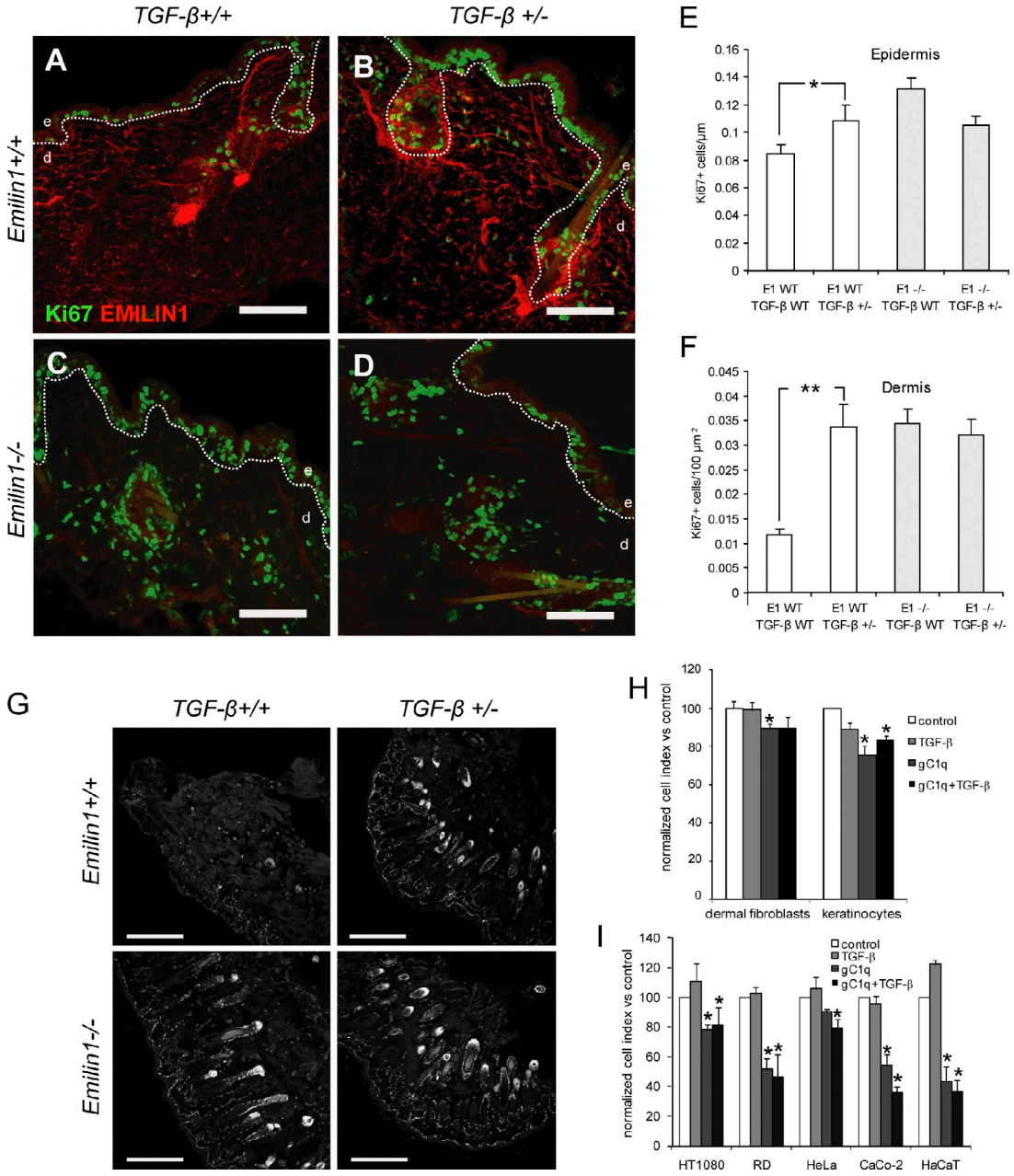

Figure S4. **EMILIN1 deficiency overrides the TGF-β effect on epidermal and dermal proliferation.** (A–D) Representative images of 7-wk-old *Emilin1*$^{+/+}$*TGF-β*$^{+/+}$, *Emilin1*$^{+/+}$*TGF-β*$^{+/-}$, *Emilin1*$^{-/-}$*TGF-β*$^{+/+}$, and *Emilin1*$^{-/-}$*TGF-β*$^{+/-}$ mouse skin cryostat sections stained for the proliferation marker Ki67. d, dermis; e, epidermis. The dashed lines denote the BM. Bars, 75 µm. (E and F) ImageJ analysis of the number of epidermal and dermal Ki67-positive cells. Mean values ± SD are reported. *, P = 0.04; **, P = 0.0001. For these quantitative analyses, three different skin cryostat sections of each mouse genotype (n = 3) were examined. (G) Representative images of 7-wk-old *Emilin1*$^{+/+}$*TGF-β*$^{+/+}$, *Emilin1*$^{+/+}$*TGF-β*$^{+/-}$, *Emilin1*$^{-/-}$*TGF-β*$^{+/+}$, and *Emilin1*$^{-/-}$*TGF-β*$^{+/-}$ mouse whisker follicle cryostat sections stained for the proliferation marker Ki67 (gray). Bars, 300 µm. (H and I) Effect of TGF-β and 5 µg/ml soluble gC1q on dermal fibroblast, keratinocyte, and cell line (HT1080, RD, HeLa, CaCo-2, and HaCaT) proliferation monitored using the XCELLigence system. The normalized cell index after 48 h of dynamic monitoring calculated as the mean ± SD from n = 3 experiments with n = 6 replicates is reported. The control corresponds to the absence of both gC1q and TGF-β. *, P < 0.05.

Reference

Verdone, G., R. Doliana, A. Corazza, S.A. Colebrooke, P. Spessotto, S. Bot, F. Bucciotti, A. Capuano, A. Silvestri, P. Viglino, et al. 2008. The solution structure of EMILIN1 globular C1q domain reveals a disordered insertion necessary for interaction with the alpha4beta1 integrin. *J. Biol. Chem.* 283:18947–18956. http://dx.doi.org/10.1074/jbc.M801085200